The University of
Nottingham

UNITED KINGDOM · CHINA · MALAYSIA

Song, Mengjie and Xia, Liang and Deng, Shiming (2016) A modeling study on alleviating uneven defrosting for a vertical three-circuit outdoor coil in an air source heat pump unit during reverse cycle defrosting. Applied Energy, 161 . pp. 268-278. ISSN 0306-2619

Access from the University of Nottingham repository:

http://eprints.nottingham.ac.uk/47514/1/A%20modeling%20study%20on%20alleviating%20uneven%20defrosting%20for%20a%20vertical%20three-circuit%20outdoor%20coil%20in%20an%20air%20source%20heat%20pump%20unit%20during%20reverse%20cycle%20defrosting.pdf

A note on versions:

The version presented here may differ from the published version or from the version of record. If you wish to cite this item you are advised to consult the publisher's version. Please see the repository url above for details on accessing the published version and note that access may require a subscription.

For more information, please contact eprints@nottingham.ac.uk

A modeling study on alleviating uneven defrosting for a vertical three-circuit outdoor coil in an air source heat pump unit during reverse cycle defrosting

Song Mengjie [a,b], Xia Liang [c,*], Deng Shiming [b]

[a] Guangdong Provincial Key Laboratory on Functional Soft Condensed Matter, School of Materials and Energy, Guangdong University of Technology, Guangzhou, China
[b] Department of Building Services Engineering, The Hong Kong Polytechnic University, Kowloon, Hong Kong Special Administrative Region
[c] Department of Building Services Engineering and Building Physics, Faculty of Science and Engineering, The University of Nottingham Ningbo China, Ningbo, China

HIGHLIGHTS

- A modeling study on better defrosting performance for an ASHP unit was reported.
- Three study cases of varying heat supply to outdoor unit were included.
- Defrosting energy consumption was decreased in all the three study cases.
- The best defrosting performances and the shortest duration were both considered.
- Energy use for defrosting could be decreased to 96.4%, and duration reduced was 7 s.

ABSTRACT

Reverse cycle defrosting is the most widely used standard defrosting method for air source heat pump (ASHP) units. It was suggested in previous experimental studies that downwards flowing of the melted frost over a vertical multi-circuit outdoor coil in an ASHP unit has negative effects on reverse cycle defrosting performance. To quantitatively study the negative effects, an experimental study and a modeling study on draining away locally the melted frost for an experimental ASHP unit with a three-circuit outdoor coil were carried out and separately reported. However, for exiting ASHP units, it is hardly possible to install water collecting trays between circuits. To alleviate uneven defrosting for a vertical multi-circuit outdoor coil in an existing ASHP unit, an effective alternative is to vary the heat supply to each refrigerant circuit by varying the opening values of modulating valves installed at an inlet pipe to each circuit. In this paper, a modeling study on varying heat (via refrigerant) supply to each refrigerant circuit in a three-circuit outdoor coil to alleviate uneven defrosting is reported. Finally, in the designed three study cases, defrosting energy use could be decreased to 94.6%, as well as a reduction of 7 s in defrosting duration by fully closing the modulating valve on the top circuit when its defrosting terminated.

1. Introduction

The development of air conditioning and heat pump technology is a natural consequence to both pursuing high quality living and working environment, and at the same time addressing the issue of sustainability. One obvious advantage for using a heat pump unit is that it can provide heating or cooling from one single machine without any major modification [1]. Air source heat pump (ASHP) units used as cooling or heating source for building heating, ventilating and air conditioning installations have been increasingly and widely applied over the recent decades in many parts of the world [2,3]. However, when an ASHP unit operates at a low temperature and high humidity environment, frost can be formed and accumulated over the surface of its outdoor coil [4,5]. The outdoor coil is usually of multi-circuit structure on the refrigerant side in order to minimize its refrigerant pressure loss and enhance the heat transfer between refrigerant and outdoor air [4–17]. Frosting adversely affects the operational performance and hence the energy efficiency of an ASHP unit, therefore periodic defrosting is necessary [6].

Defrosting could be realized by a number of methods including: (1) compressor shut-down defrosting [18], (2) electric heating defrosting [19,20], (3) hot water spray defrosting [7], and (4) hot

gas by-pass defrosting [21–25]. Currently, reverse cycle defrosting is the most widely standard defrosting method used for ASHP units [5,8–17,26–28]. During reverse cycle defrosting, a space heating ASHP unit actually cools a space, degrading indoor thermal comfort while consuming electrical energy for melting frost [9]. Therefore, a defrosting period should be controlled to as short as possible [10,11]. In order to better improve the defrosting performance for an ASHP unit, a number of previous experimental studies were carried out to exam various ways for better defrosting performances. These included optimizing the structure of an evaporator [12,29], fin space adjustment [30], fin surface treatment [31], heating up the liquid refrigerant in an accumulator [32], providing heat for defrosting using phase change materials [9,13], etc.

Among these exploratory experimental studies on improving system defrosting performance, for ASHP units with vertical multi-circuit outdoor coils, the phenomenon that different circuits terminate their defrosting processes at different time was found and reported. For example, O'Neal et al. [28] and Qu et al. [14] both investigated the transient defrosting performances of ASHP units, each with a vertical four-circuit outdoor coil. It was reported that when a defrosting process was terminated, the surface temperature at the exit of the lowest circuit was much lower than that at the exit of the highest circuit. Similar phenomenon could also be found in Wang's study [15]. In this paper, to clearly describe this phenomenon, it was defined as uneven defrosting. For an ASHP unit with a vertical multi-circuit outdoor coil, defrosting operation is always terminated when the tube surface temperature at the exit of the lowest circuit reaches a pre-set temperature [12–15,17,21–24,30,31]. Therefore, uneven defrosting is that the tube surface temperatures at exits of each circuit reach the pre-set temperature at different time. To explore the reason that results in the uneven defrosting, for a vertical multi-circuit outdoor coil in an ASHP unit, it was demonstrated [14] that downwards flowing of the melted frost due to gravity from up circuit(s) would adversely affect the defrosting performance of down circuit(s).

On the other hand, an effective alternative to experimentally studying the defrosting performance in an ASHP unit is via numerical approach and therefore, the last two decades saw a growing number of modeling studies [16,17,23–27] on defrosting operations. Noticeable, Krakow et al. firstly developed a hot gas defrosting model for evaporators [23,24], and later presented an idealized reverse cycle defrosting model for an ASHP unit with a receiver [26,27]. Dopazo et al. also developed a detailed transient simulation model for hot-gas bypass defrosting in an air-cooled evaporator [25]. In the above mentioned defrosting models, the effects of downwards flowing of the melted frost due to gravity along the surface of a multi-circuit outdoor coil on the defrosting performance all were neglected, by assuming either no water retention on coil surface or a stable water layer. Only the semi-empirical model developed by Qu et al. considered the negative effects of melted frost [16]. Thereafter, as a follow-up to Qu's study on uneven defrosting, a recent experimental and modeling study on the defrosting performance of an ASHP unit when the melted frost was drained away locally from its three-circuit outdoor coil were carried out and separately reported [11,17].

While the outcomes from these studies [11,17] demonstrated the effectiveness of locally draining away the melted frost from a vertical multi-circuit outdoor coil, for existing ASHP units, however, it is hardly possible to install water collecting trays between circuits. Nonetheless, for existing ASHP units, it is still possible to vary the heat input to each refrigerant circuit through varying refrigerant supply to each circuit [33]. This is because uneven defrosting was fundamentally caused by different thermal loads imposed to each circuit due to the downwards flowing of the melted frost, when the supply of refrigerant or heat to each circuit was the same. Consequently, if the heat to be supplied to each circuit may be var-

ied according to the actual defrosting thermal load each circuit is to deal with, then the problem of uneven defrosting may be alleviated. Modulating valves installed at an inlet refrigerant pipe to each circuit may be deployed to vary the refrigerant flow thus heat input to each circuit. Therefore, in this paper, a modeling study on varying heat (via refrigerant) supply to each refrigerant circuit in the three-circuit outdoor coil [11,17] to alleviate uneven defrosting is carried out and reported. Firstly, the methodology and three study cases are explained. Secondly, the results of the modeling study on defrosting durations and energy use in the three study cases are presented. Finally, a conclusion is given.

2. Methodology and study cases

The reported study was carried out using a previously developed and validated semi-empirical mathematical model at the experimental setting of without using water collecting trays between circuits [11]. In this Section, a brief description of the previous experimental study is firstly introduced, and the validated models are then shown. This is followed by presenting three study cases in this study. Finally, the assumptions used for the three study cases will be given.

2.1. Experimental study

To quantitatively study the negative effects of downwards flowing of the melted frost during reverse cycle defrosting, an experimental ASHP unit with a vertical three-circuit outdoor coil was specifically established. It was modified from a commercially available 6.5 kW heating-capacity variable speed ASHP unit. The experimental ASHP unit was installed in an existing environmental chamber having a simulated heated indoor space and a simulated outdoor frosting space. The sizes of both spaces were each measured at 3.8 m (L) × 3.8 m (W) × 2.8 m (H). Fig. 1 shows the schematics of the ASHP unit installed in the environmental chamber. The experimental ASHP unit was a split-type one, consisting of a swing type compressor, an accumulator, a four-way valve, an electronic expansion valve, an indoor coil and an outdoor coil. The outdoor coil was specially designed and made, as shown in Fig. 2. There were three individual and parallel refrigerant circuits and the airside surface areas corresponding to each of the three circuits were the same. The outdoor coil was vertically installed, and in each circuit a solenoid modulating valve and a manual stop valve were used. The specifications of the three-circuit outdoor coil are shown in Table 1.

The experimental conditions were jointly maintained by the use of a separate air conditioning system in the environmental chamber, and sensible and latent load generating units (LGUs) which were used to simulate thermal load. During normal heating (or frosting) operation, a frosting environment in the outdoor space was maintained by running the experimental ASHP unit and LGUs together, while an indoor heated environment by the experimental ASHP unit and the existing air conditioning system. All the parameters, such as temperature, pressure, relative humidity, refrigerant mass flow rate, voltage and current, were measured. All sensors and measuring devices were able to output direct current signals of 4–20 mA or 1–5 V to a data acquisition system (DAS) for logging and recording. All the measured data throughout both frosting and defrosting periods were collected and recorded by the DAS at an interval of 5 s. In addition, during defrosting, photos for surface conditions of the outdoor coil were taken at an interval of 10 s.

Three cases were designed and carried out in this experimental study, and two of them were prototypes of the following models developed. For Case 1, there was no water collecting trays installed between circuits, as shown in Fig. 2(a). During defrosting, the
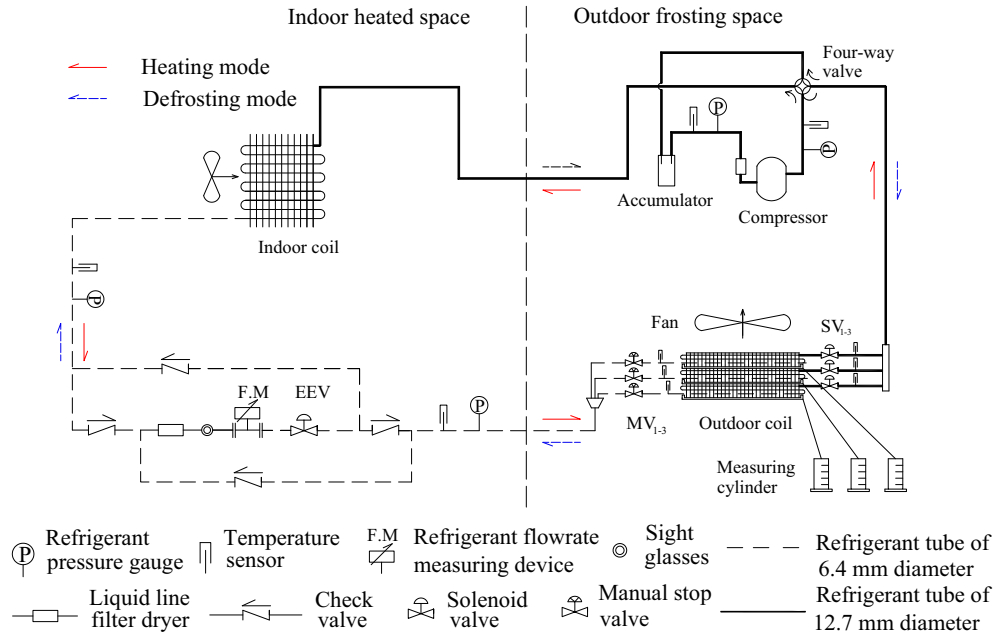
Fig. 1. Schematics of the ASHP unit with a vertical three-circuit outdoor coil.

melted frost could downwards flow from up circuit(s) to down circuit(s) freely due to gravity. As shown in Fig. 2(b), for Case 3, there were two water collecting trays (Tray A and Tray B) installed between circuits. The melted frost would be taken away when it was downwards flowing away from the circuit during defrosting, and thus the negative effects of melted frost were eliminated. The experimental results were compared, and the negative effects of downwards flowing melted frost were qualitatively studied. At the same time, water collecting tray was suggested to install between circuit for a multi-circuit outdoor coil when optimizing its structure, and thus improving system defrosting performance. On the other hand, more information was obtained from this experimental study. Firstly, all the data used in the following modeling development as known parameters were collected, such as the tube surface temperature at the inlet of each refrigerant circuit, the refrigerant mass flow rate and the total mass of melted frost collected. Secondly, part of the experimental results would be used in the validation stage of the following two developed models.

However, there are still some limitations in this experimental study. Firstly, some parameters could not be measured, such as the rate of melted frost downwards flowing along the surface of outdoor coil. Secondly, some parameters, like the temperature of melted frost when it was downwards flowing, were hardly impossible to be measured. Thirdly, some parameters were easy to measure, but not accurate due to their fluctuations, such as the temperature of air around the outdoor coil. In the experimental study, this type of parameters was always measured by many sensors or tested by many times. Therefore, the following modeling study takes the responsibility to measure the previous three types of parameters.

2.2. Modeling study

The development of the validated semi-empirical model at the setting of without using water collecting trays between circuits for the experimental ASHP unit was separately reported previously [17]. However, for the completeness of the current paper, it is briefly described here. The prototype of this model was Case 1 in the previous experimental study. Details of the vertical three-circuit outdoor coil without water collecting tray installed between

circuits were shown in Fig. 2(a), and conceptual model for the airside of the three-circuit outdoor coil shown in Fig. 3. Before the model was built, series of assumptions were given, such as the frost at the surface of each circuit was even, and the refrigerant mass flow evenly distributed, and so on. At the same time, as mentioned at previous, some of experimental results obtained were used as known parameters when the model was developed.

In this model, a defrosting process on the airside of the outdoor coil was divided into four stages: (1) preheating, (2) frost melting without water flowing away from a circuit, (3) frost melting with water flowing away from a circuit, and (4) water layer vaporizing. Schematics of mass and energy flows in the four defrosting stages were shown in Fig. 4. Moreover, as part of the entire setup of the three-circuit outdoor coil, a mathematical sub-model for the heat and mass flows on a water collecting tray and a water collecting cylinder was also developed, and used together with the model. As shown in Fig. 5, there were three steps for the process of the mass and energy flows in a water collecting tray during defrosting.

During the modeling study, 42 equations were used [17]. Although the models were developed based on energy and mass flows conservations, there existed a few limitations. Those included the assumptions introducing errors, certain empirical formulas having their limitations, and experimental data making the models empirical. Therefore, appropriate modifications might have to be introduced when the models are to be used for studying ASHP units with different configurations or operating conditions. After this model was built, it was validated by comparing the predicted defrosting duration, tube surface temperatures at the exit of each circuit, temperature variations of the melted frost and the total mass of the melted frost collected in a Measuring Cylinder shown in both Figs. 1 and 2(a), with the corresponding experimental data [11,17]. The average deviations between measured and predicted results of tube surface temperatures at exits of Circuits 1–3 were −0.2 °C, 0 °C and 0.4 °C, respectively. The maximum and average deviations between the measured and the predicted results of the temperature variations of the melted frost were 0.68 °C and 0.05 °C, respectively. Finally, the difference between the measured and predicted total melted frost mass was only 0.2%. Therefore, this validated model at the setting of without using water collecting trays between circuits could adequately describe the defrosting
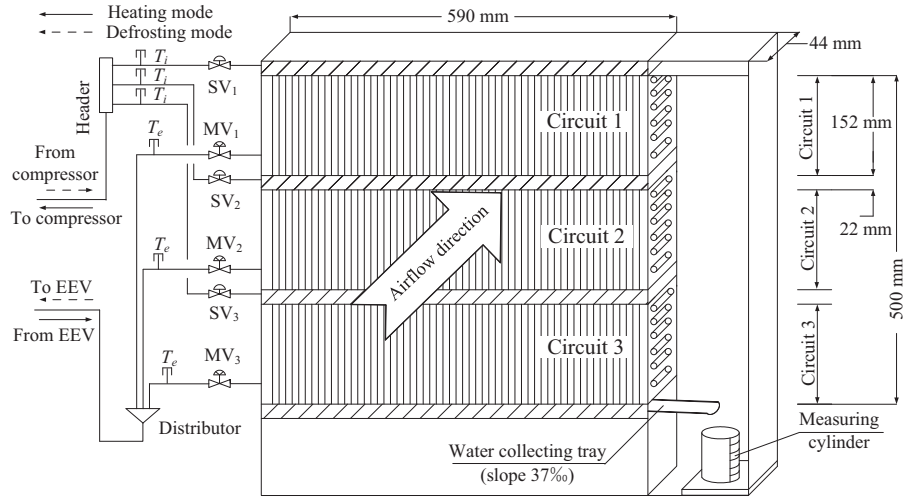
(a) Without water collecting tray installed between circuits (Case 1 in Re[11])
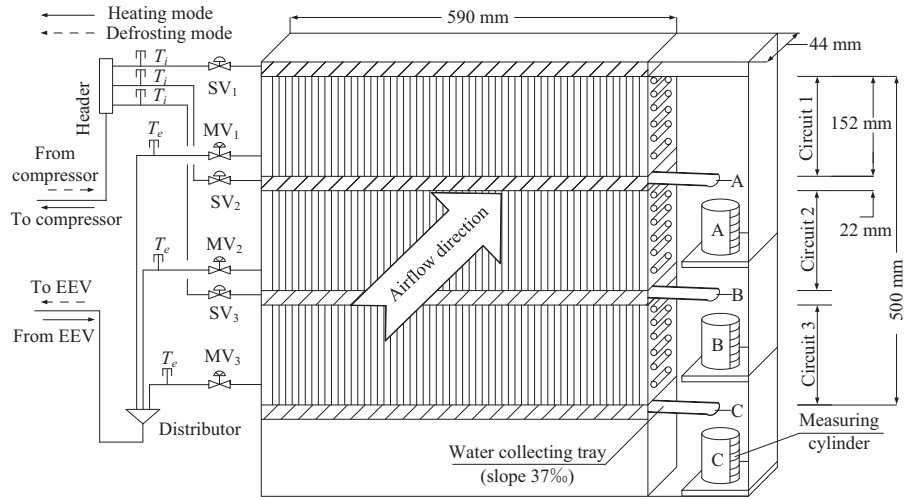
(b) With water collecting tray installed between circuits (Case 3 in Re[11])

Fig. 2. Details of the vertical three-parallel refrigerant circuit outdoor coil without and with water collecting tray installed between circuits.

Table 1
Specifications of the specially designed outdoor coil and the water collecting components.

Item	Parameter	Value	Unit
1	Height of the outdoor coil	500	mm
2	Width of the outdoor coil	590	mm
3	Thickness of the outdoor coil	44	mm
4	Fin height	152.4	mm
5	Fin width	44	mm
6	Fin thickness	0.115	mm
7	Fin pitch	2.1	mm
8	Tube external diameter	10	mm
9	Tube thickness	0.5	mm
10	Tube spacing	20	mm
11	Number of tube rows	2	–
12	Number of circuits	3	–
13	Number of water collecting trays	3	–
14	Number of water collecting cylinders	3	–
15	Circuit pitch	22	mm
16	Tube material	Copper	–
17	Fin material	Aluminum	–
18	Fin type	Plate	–
19	Water collecting tray material	PVC	–
20	Water collecting cylinder material	PVC	–
21	Volume of the water collecting cylinder	500	mL

performance for the experimental ASHP unit and was used in the current modeling study.

2.3. The three study cases

When an ASHP unit operates at defrosting mode, usually the refrigerant discharged from compressor is assumed equally dis-
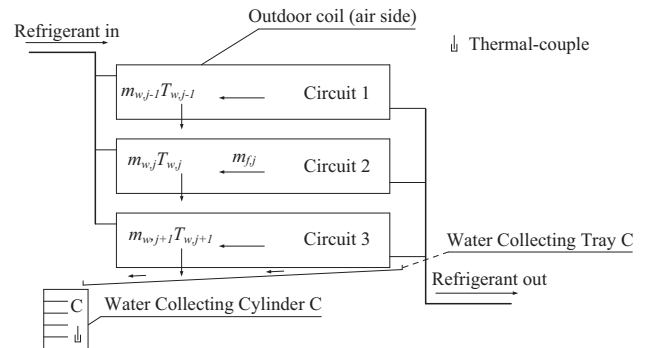

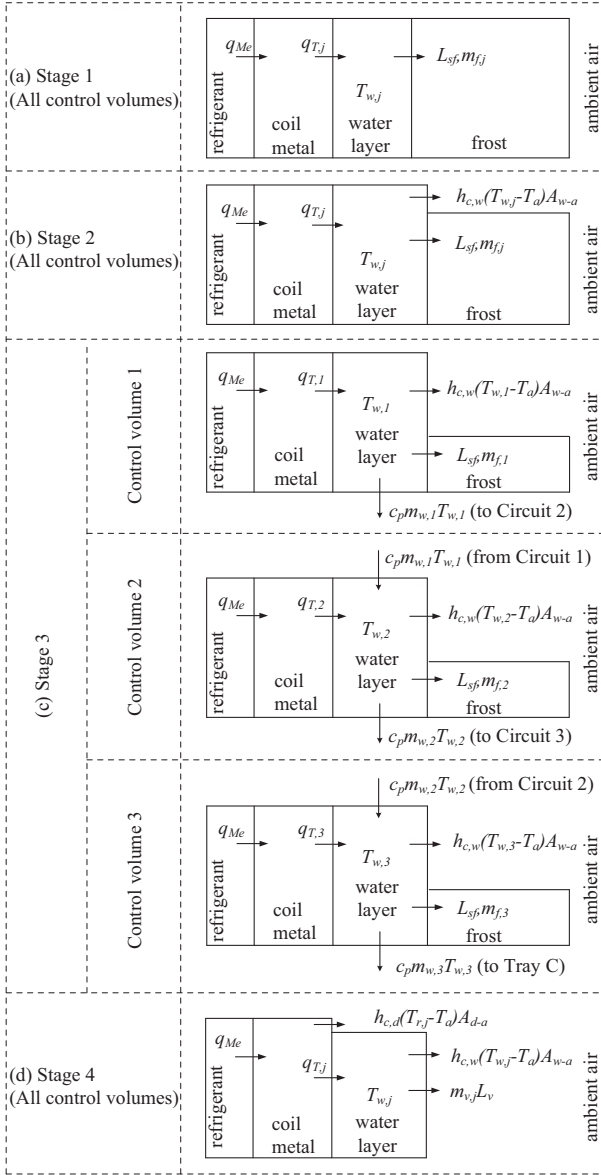**Fig. 3.** Conceptual model for the airside of the three-circuit outdoor coil.

4

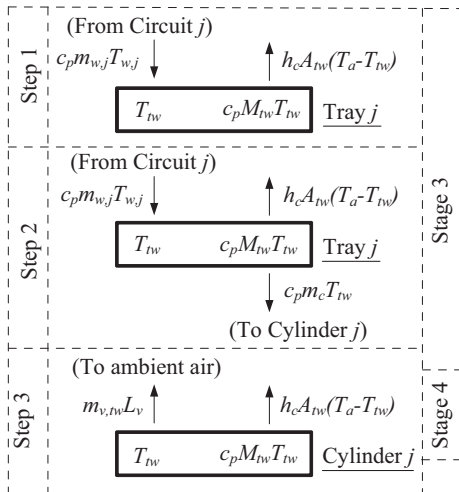Fig. 4. Schematics of mass and energy flows in the four defrosting stages (Ref. [17]).

Fig. 5. Schematics of mass and energy flows in a water collecting tray and a water collecting cylinder during defrosting.

tributed into each circuit of a multi-circuit outdoor coil. As shown in Fig. 6, the refrigerant mass flow rates in the three circuits during defrosting in the previous experimental study were calculated. From 0 s to 70 s, the refrigerant mass flow rates were fluctuating, named Stage 1 in this study. At Stage 2, from 70 s to 160 s, their values increased steadily, with their peak values at 10.52 g/s at 160 s into defrosting. The following period was named Stage 3, and the refrigerant mass flow rate decreased firstly, and then kept fluctuating to the termination of defrosting. It could be found that, the refrigerant mass flow rates of the three circuits calculated kept the same always during defrosting. However, as the melted frost flows downwards along the surface of outdoor coil due to gravity, the heating load for each refrigerant circuit becomes different. In this study, therefore, to alleviate the uneven defrosting due to the downwards flowing of melted frost for the three-circuit vertical outdoor coil during reverse cycle defrosting, three study cases were included where different openings of modulating valves were applied so as to vary the heat supply to each of the three circuits. Table 2 details the opening of modulating valve and other operational changes in the three study cases. At the same time, to clearly describe their differences, changes in the proportion of the refrigerant distribution into each circuit in the three study cases were illustrated in Fig. 7.

2.3.1. Case 1

Fig. 8 shows the measured tube surface temperature at the exit of each circuit during defrosting in the previous experimental study in Case 1 in Ref. [11]. It could be seen that the temperature order of three circuits kept at $T_1 > T_2 > T_3$ during defrosting. This
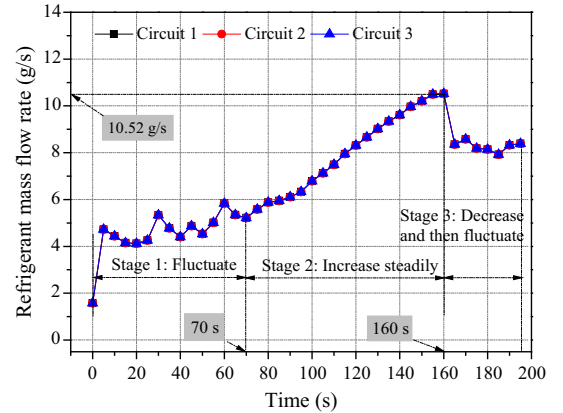

Fig. 6. Calculated refrigerant mass flow rate in the three circuits during defrosting in the previous experimental study.

is because of the negative effects of the downwards flowing melted

Table 2
Experiment conditions in the three study cases.

Case No.	Opening of modulating valve	Other operational changes	Refrigerant changes shown in
Case 1	A	None	Figs. 7(a) and 9
Case 2	B	None	Figs. 7(b) and 10
Case 3	C	D	Figs. 7(c) and 11

A. The opening values of three valves on each circuit, from top to bottom, were fixed at 92.5%, 97.8% and 100%, respectively.
B. Fully open all valves at the start of defrosting, and fully close the modulating valve on Circuit 1 when its defrosting was terminated.
C. Fully open all valves at the start of defrosting, and fully close the modulating valve on Circuit 1 when its defrosting was terminated.
D. Keep the refrigerant flows to Circuit 2 and Circuit 3 unchanged by reducing compressor speed to 66.7% of the original speed when the modulating valve on Circuit 1 is closed.
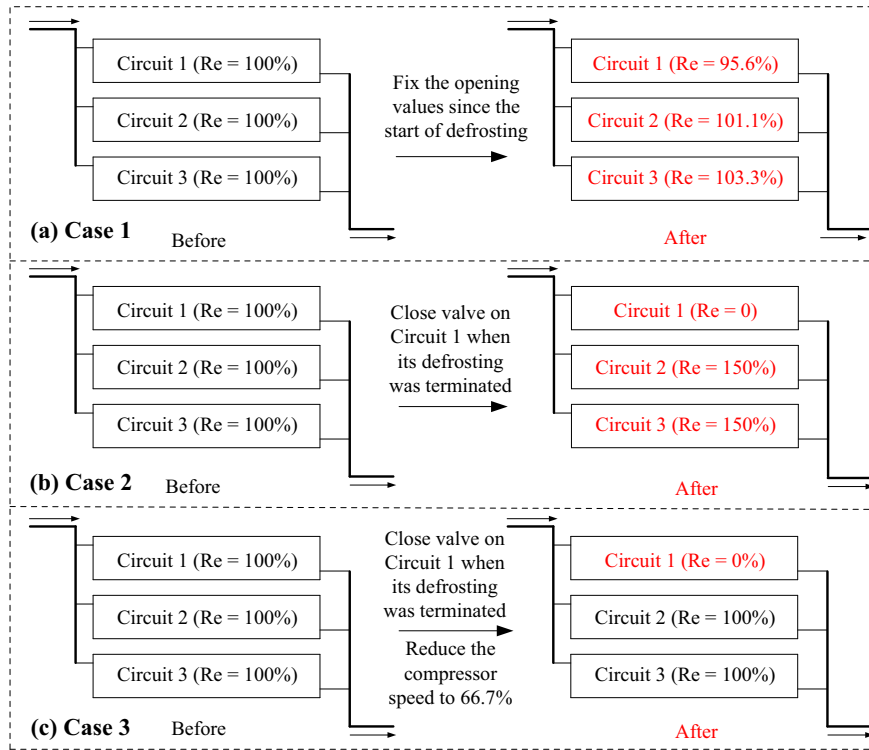
Fig. 7. Changes in the proportion of the refrigerant distribution into each circuit in the three study cases.
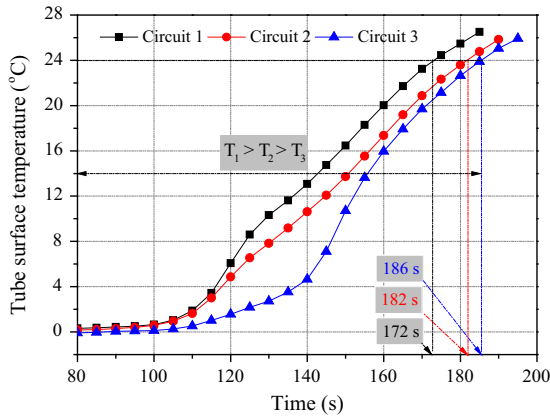

Fig. 8. Measured tube surface temperature at the exit of each circuit during defrosting in the previous experimental study (Case 1 in Ref. [11]).

Fig. 9. Assumed refrigerant mass flow rate in the three circuits during defrosting in Study Case 1.

frost. Experimental results shown that the defrosting durations for the 3 circuits, from top to bottom, were 172 s, 182 s, and 186 s, respectively [11]. In other words, the defrosting durations for the top and the middle circuits were 92.5% and 97.8%, respectively, of that for the bottom circuit. To alleviate the uneven defrosting, Study Case 1 was then designed, where the modulating valve for the bottom circuit was fully opened and the openings of the modulating valve for the top and middle circuits were set at 92.5% and 97.8% of full opening, respectively. In this way, the heat supplies to the three circuits via the supply of refrigerant during defrosting were no longer the same, and the assumed refrigerant mass flow rates to each circuit during defrosting are 95.6%, 101.1%, and 103.3% of their previous values, respectively, as shown in Fig. 7.

Fig. 9 shows the assumed refrigerant mass flow rate in the three circuits during defrosting in Study Case 1. The trends of refrigerant mass flow rates in the three circuits during defrosting at three
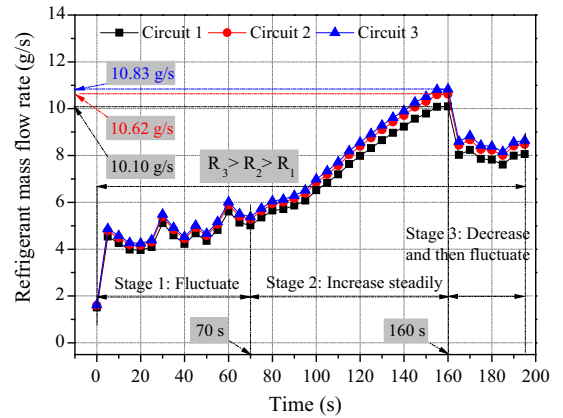
stages are the same as those shown in Fig. 6. However, their peak values, at 160 s into defrosting, were 10.10 g/s for Circuit 1, 10.62 g/s for Circuit 2, and 10.83 g/s for Circuit 3, respectively. During defrosting, the mass flow rate order was always at $R_3 > R_2 > R_1$, which met the designed experiment conditions in Table 2 and the changes in the proportion of the refrigerant distribution shown in Fig. 7(a).

2.3.2. Case 2

As shown in Fig. 8, the results from the previously experimental study also revealed that the defrosting duration for Circuit 1 was the shortest [11]. Hence, it was also possible to vary the heat input to the three refrigerant circuits by fully closing the modulating valve on Circuit 1 when its tube surface temperature at exit reached 24 °C, which means its defrosting process was terminated. Therefore, in Study Case 2, it was designed that the three valves on

6

the three circuits were fully open at the start of defrosting. When the defrosting of Circuit 1 was terminated, the modulating valve on it would be fully closed. Consequently, more refrigerant would flow into the other two refrigerant circuits to speed up their defrosting. Fig. 7(b) illustrates the changes in the proportion of the refrigerant distribution into each circuit, and Fig. 10 shows the assumed refrigerant mass flow rates to each circuit during defrosting in Study Case 2. It could be found that the trends of refrigerant mass flow rates in the three circuits during defrosting at Stages 1 and 2 are the same as those shown in Fig. 6. But at Stage 3, the refrigerant mass flow rate of Circuit 1 decreased to 0 g/s at 172 s, as designed in Table 2. At the same time, the values of the other two circuits increased firstly, and then kept fluctuating, with their same peak values at 12.59 g/s at 195 s into defrosting. All their trends met the changes in the proportion of the refrigerant distribution shown in Fig. 7(b).

2.3.3. Case 3

As shown in Figs. 7(b) and 10, in Study Case 2, when the modulating valve on Circuit 1 was closed, the refrigerant mass flow rates to the other two circuits were increased. To possibly reduce defrosting energy consumption, however, it was possible to decrease compressor speed so that the refrigerant flow rates to Circuit 2 and Circuit 3 remained unchanged. Therefore, in Study Case 3, it was designed that the three modulating valves on the three circuits were fully open at the start of defrosting. When the tube surface temperature at the exit of Circuit 1 reached 24 °C, its modulating valve would also be fully closed, the same as that in Study Case 2. However, compressor speed was also reduced by 1/3 at the same time. The changes in the proportion of refrigerant distribution into each circuit during defrosting in Study Case 3 were shown in Fig. 7(c), and the assumed refrigerant mass flow rates to each circuit are shown in Fig. 11. The same as that shown in Fig. 10, the trends of refrigerant mass flow rates in the three circuits during defrosting at Stages 1 and 2 are the same as those shown in Fig. 6. In addition, at Stage 3, the refrigerant mass flow rate of Circuit 1 decreased to 0 g/s at 172 s, as designed in Table 2. At the same time, the values of other two circuits increased firstly, and then kept fluctuating, with their same peak values at 12.59 g/s at 195 s into defrosting. All their trends met the changes in the proportion of the refrigerant distribution shown in Fig. 7(c).

2.4. The seven assumptions

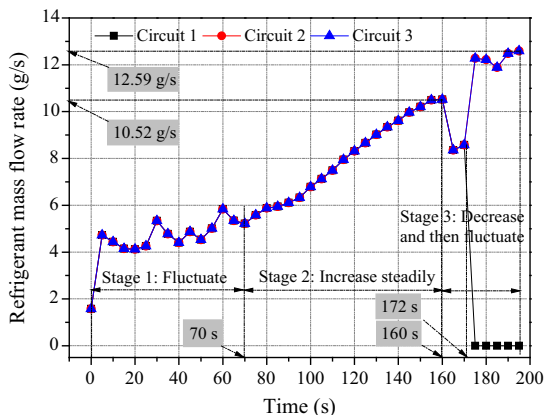In the current modeling study, the following were also assumed:

Fig. 10. Assumed refrigerant mass flow rate in the three circuits during defrosting in Study Case 2.
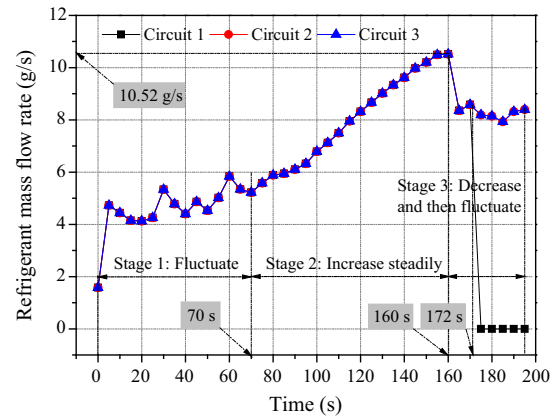

Fig. 11. Assumed refrigerant mass flow rate in the three circuits during defrosting in Study Case 3.

(i) In the previous experimental study, the refrigerant mass flow rate in the three refrigerant circuits was assumed evenly distributed. The calculated refrigerant mass flow rates in the three circuits in the previous experimental study were derived following this assumption.

(ii) In the three study cases, the refrigerant mass flow rate passing through a modulating valve to each circuit during defrosting was assumed to be proportional to the respective percentage openings of the three modulating valves, under a constant total refrigerant flow rate. For example, when the percentage openings of valves are 50% for the valve on Circuit 1, 100% for the valves on Circuit 2 and Circuit 3, respectively, the ratio of the three valves' openings is 1:2:2, and thus the percentage shares of the total refrigerant mass flow rate passing through the three modulating valves are 20%, 40%, and 40%, respectively. The assumed refrigerant mass flow rates to each circuit during defrosting in Study Case 1 shown in Figs. 7(a) and 9 were derived following this assumption.

(iii) In Study Case 2, the total refrigerant mass flow was evenly distributed to the other two refrigerant circuits during defrosting after the modulating valve on Circuit 1 was closed. As a result, the refrigerant mass flow rate to Circuit 2 and Circuit 3 was each increased by 50%, as illustrated in Fig. 7(b).

(iv) In Study Case 3, as the modulating valve on Circuit 1 was closed, the refrigerant mass flow in Circuit 2 and Circuit 3 remained unchanged, as a result of compressor speed reduction by 33%.

(v) The energy consumption on compressor would decreased 33%, as a result of compressor speed reduction by 33%.

(vi) When the tube surface temperature at the exit of a refrigerant circuit reached 24 °C, the defrosting operation on that circuit was considered ended. The experiment conditions illustrated in Fig. 7(b) and (c) were derived following this assumption.

(vii) The defrosting duration for the ASHP unit was the same as that of Circuit 3.

3. Results

Using the validated empirical model [17], a modeling study for the three study cases was undertaken and the study results are shown in Figs. 12–14 for the three study cases. In addition, to illustrate the effectiveness of varying heat supply to respective refrigerant circuit, the results of previous experimental study [11] for the
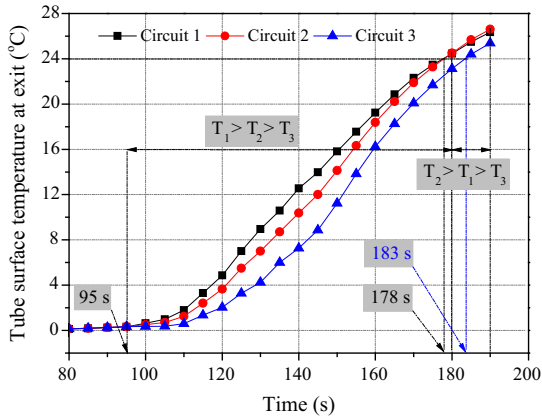
Fig. 12. Predicted tube surface temperatures at circuit exits during defrosting in Study Case 1.
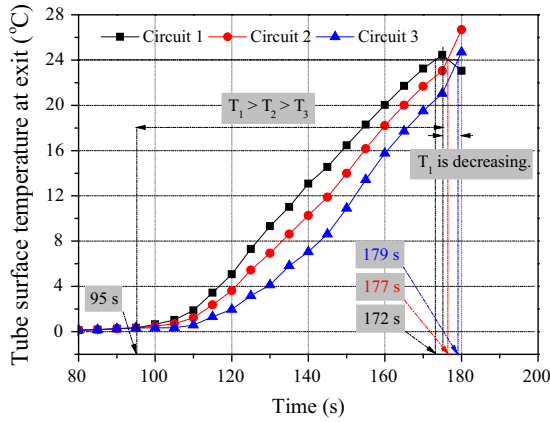

Fig. 13. Predicted tube surface temperatures at circuit exits during defrosting in Study Case 2.
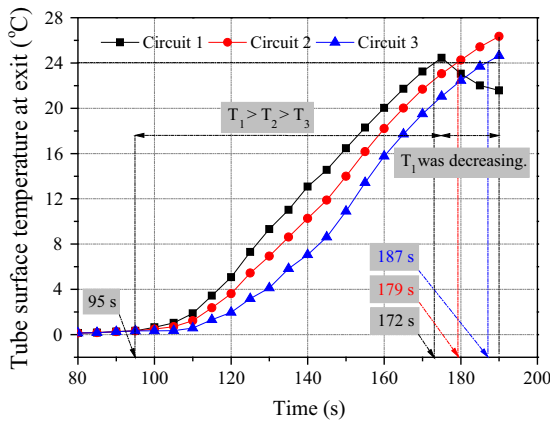

Fig. 14. Predicted tube surface temperatures at circuit exits during defrosting in Study Case 3.

setting of without using water collecting trays between circuits [17] shown in Fig. 8 were also used for comparison purposes. In Figs. 8 and 12–14, for their time (horizontal) axis, although defrosting starts at 0 s, 80 s is the chosen time point for these figures in order to more clearly show the temperature rise during defrosting. Further, Table 3 summarizes the defrosting durations in the previous experimental study and the three study cases. For the results

Table 3
Defrosting durations in the previous experimental study and the three study cases.

Case No.	Defrosting durations for each circuit			Shown in
	Circuit 1 (s)	Circuit 2 (s)	Circuit 3 (s)	
Experimental study	172	182	186	Figs. 8 and 15
Study Case 1	178	178	183	Figs. 12 and 15
Study Case 2	172	177	179	Figs. 13 and 15
Study Case 3	172	179	187	Figs. 14 and 15

presented here in the three study cases, the time difference in defrosting duration between Circuit 1 and Circuit 3, Δt, was used as a parameter to indicate the degree of uneven defrosting. The smaller the value of Δt was, uneven defrosting was eliminated much more effectively.

3.1. Case 1

Fig. 12 shows the variations of the predicted tube surface temperatures at the exit of each circuit during defrosting in Study Case 1. It can be seen that the defrosting durations were 178 s for Circuit 1 and Circuit 2, and 183 s for Circuit 3, respectively. From 95 s to 180 s into defrosting, the temperature order of the three circuits kept at $T_1 > T_2 > T_3$. However, the temperature order changed to $T_2 > T_1 > T_3$ after 180 s into defrosting, because the refrigerant mass flow rate distributed into Circuit 1 was less than those in others. This phenomenon met the changes in the proportion of the refrigerant distribution into each circuit in the Study Case 1, as shown in Figs. 7(a) and 9. It also can be found that the defrosting durations for Circuit 2 and Circuit 3 were shortened, but that for Circuit 1 was slightly extended, as compared to the experimental results shown in Fig. 8. This was because the refrigerant supply to each circuit was no longer the same. Following the Assumption (ii) specified in Section 2.4, as shown in Figs. 7(a) and 9, the refrigerant mass flow rate during defrosting in Circuit 1 is decreased to 95.6% of previous value, and that in Circuits 2 and 3 increased to 101.1% and 103.3% of previous values, respectively. Compared to the results from the previous experimental study [11], the defrosting duration for Circuit 3 or the ASHP unit was decreased by 3 s, or ~1.6%. Also, as seen, Δt was 5 s, which is much shorter than the experimental value of 14 s, suggesting that the uneven defrosting was significantly alleviated.

3.2. Case 2

Fig. 13 shows the variations of the predicted tube surface temperatures at the exit of each circuit during defrosting in Study Case 2. The simulation results demonstrated that the defrosting for durations were 172 s for Circuit 1, 177 s for Circuit 2, and 179 s for Circuit 3, respectively. From 95 s to 175 s into defrosting, the temperature order of the three circuits kept at $T_1 > T_2 > T_3$. When the tube surface temperature at the exit of Circuit 1 reached 24 °C at 173 s into defrosting, its modulating valve was closed, so that, the refrigerant supply to Circuit 1 was reduced to 0 g/s, as shown in Figs. 7(b) and 10. At the same time, since the compressor speed remained unchanged, the refrigerant supplies to Circuit 2 and Circuit 3 were consequently increased to 150% of previous values. As a result of the increase in refrigerant mass flow rate, it can be seen from Fig. 13 that the tube surface temperatures were increased for Circuit 2 and Circuit 3, but decreased for Circuit 1 after closing valve, from 175 s into defrosting to the termination. Compared to the results of the previous experimental study [11], the defrosting duration for Circuit 3 or the ASHP unit was decreased by 7 s, or about 3.8%. The value of Δt was 7 s, also suggesting the alleviated uneven defrosting.
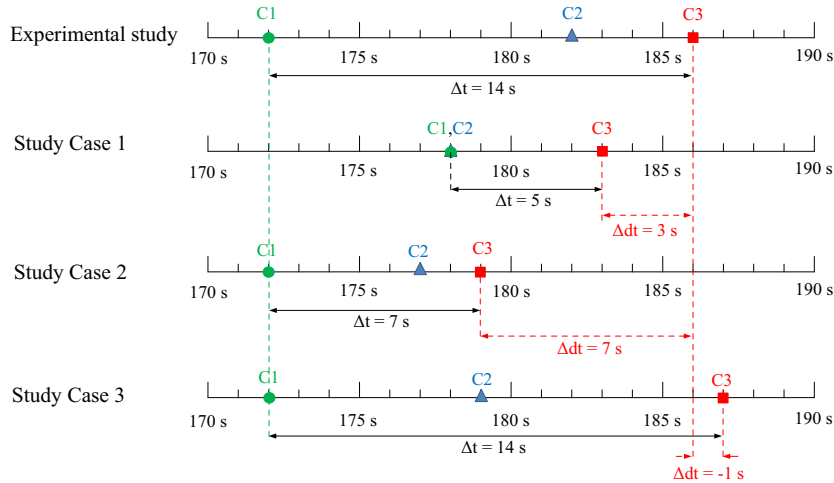
8

Fig. 15. Analysis on durations for the previous experimental study and the three study cases.

3.3. Case 3

Fig. 14 shows the variations of the predicted tube surface temperatures at the exit of each circuit during defrosting in Study Case 3. The simulation results showed that the defrosting durations were 172 s for Circuit 1, 179 s for Circuit 2, and 187 s for Circuit 3, respectively. As shown in Figs. 7(c) and 11, when the modulating valve on Circuit 1 was closed at 172 s into defrosting, its refrigerant mass flow rate was reduced to 0 g/s. For the other two circuits, the refrigerant mass flow rates remained unchanged after the compressor speed was reduced by 1/3. As seen, the surface temperature for Circuit 1 was reduced after closing the valve at 172 s, but those for Circuit 2 and Circuit 3 continued their increasing trend. Unlike the other two study cases, the defrosting duration for Circuit 3 or the ASHP unit was slightly increased by 1 s to 187 s, when compared with the results of the previous experimental study [11]. At the same time, Δt was also slightly increased by 1 s to 15 s, suggesting that the problem of uneven defrosting remained.

The simulation results for the three study cases are summarized in Table 3, where the results of the previously experimental study are also included. To clearly illustrate the difference of these durations, analysis on durations for the three study cases and the previous experimental and modeling studies were shown in Fig. 15. In this figure, the time difference in defrosting duration between study case and previous experimental study, Δdt, was used as a parameter to indicate the defrosting duration. The bigger the value of Δdt was, the defrosting process of this study case was terminated much earlier. It can be seen from Table 3 and Fig. 15 that for the three study cases, Study Case 2 appeared to be the better one in terms of shortening the defrosting duration with the shortest duration of 179 s, with 7 s earlier than the defrosting termination of previous experimental study. Also it can be seen from the Fig. 15 that, the values of Δt for Study Case 1 and Study Case 2 were significant smaller than the experimental value and that for Study Case 3, suggesting that using the methods in Study Cases 1 and 2 can help alleviate uneven defrosting for a better defrosting performance. However, since different defrosting durations for the three study cases were resulted in, the energy use for defrosting was therefore different. This is further discussed in Section 4.

4. Analysis on heat supply and energy consumption

For an ASHP unit, during reverse cycle defrosting, the energy is used to heat the outdoor coil metal, melt frost, heat the melted

frost, heat the cold ambient air, and evaporate the retained water on the surface of outdoor coil. In this study, the total energy use for defrosting was also evaluated for the three study cases, 715.9 kJ for Case 1, 693.2 kJ for Case 2, and 728.0 kJ for Case 3, respectively. Compared with the experimental of 732.6 kJ, the defrosting energy uses in the three study cases were all less, with that defrosting energy use in Study Case 2 being the lowest at about 94.6% of the experimental value. It is noted that in Study Case 3, compressor speed was reduced by 1/3 for possible energy saving after the tube surface temperature at the exit on Circuit 1 reached 24 °C. However, since the total durations of defrosting operation was longer than that in Study Case 2, the total energy use in Study Case 3 was more than that in Study Case 2, and slightly lower than the experimental value.

To clearly show the differences of heat supply, Fig. 16 shows the heat supply for defrosting after 172 s into defrosting in the previous experimental study and the three study cases. It is obvious that the heat supply for defrosting in Study Case 2 was shortest, at 33.8 kJ. At the same time, three study cases all could decrease the heat supply for defrosting, because the value in the previous experimental study was the biggest, at 73.2 kJ. The heat supply mostly comes from the thermal energy of indoor air, accounting of more than 86% of the total heat supply. The least part is the heat supply from supply fan, at only around 1%. In addition, energy consumption during defrosting in the previous experimental study and the three study cases is shown in Fig. 17. It could be found that energy consumption on frost melting for different study cases were
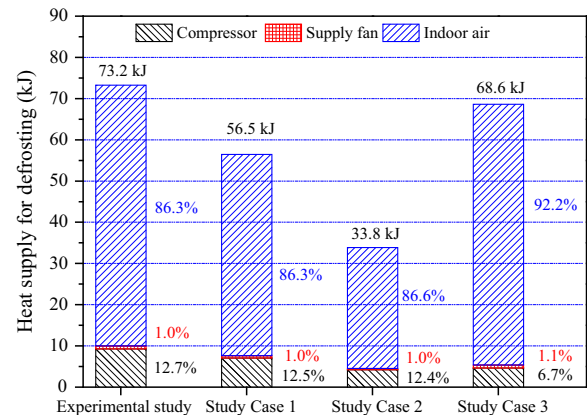

Fig. 16. Heat supply for defrosting after 172 s into defrosting in the previous experimental study and the three study cases.
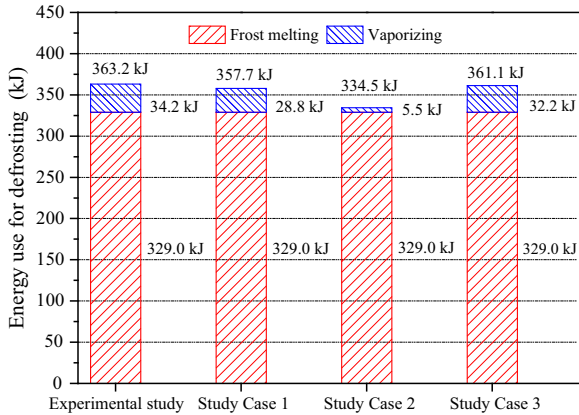
9

Fig. 17. Energy consumption during defrosting in the previous experimental study and the three study cases.

the same, at 329.0 kJ. This is because the frost accumulation on the surface of outdoor coil was assumed the same as that in the previous experimental study. The differences totally come from the energy consumption on vaporizing. The biggest value of energy consumption on vaporizing is 34.2 kJ, in the previous experimental study. And the smallest one is only 5.5 kJ, or 16.1% of the value in the previous experimental study. Figs. 16 and 17 show the heat supply for defrosting and energy consumption in the Study Case 2 both were the shortest. This further confirmed that system performance could be improved most by fully closing the modulating valve on the top circuit when its defrosting terminated in the three study cases for alleviating uneven defrosting.

5. Conclusions

A modeling study on alleviating uneven defrosting for a vertical three-circuit outdoor coil in an ASHP unit during reverse cycle defrosting was undertaken and the study results are reported. The following conclusions could be received from this paper:

(a) Three study cases were included and study results suggested that the best operating defrosting performances in terms of defrosting durations and energy use were achieved in Study Case 2. In this study case, defrosting energy use could be decreased to 94.6%, as well as a reduction of 7 s in defrosting duration by fully closing the modulating valve on the top circuit when its defrosting terminated.

(b) It is expected that with more refrigerant circuits in an outdoor coil in an ASHP, the method of fully closing the modulating valves on top circuit when its defrosting terminated will yield better defrosting performance for the ASHP unit, as predicted by the modeling study reported in this paper.

(c) In this modeling study, frost accumulation on the surface of each circuit and the refrigerant distributed into each circuit in the multi-circuit outdoor coil both were assumed even. However, when the frost accumulation and refrigerant distribution were uneven, the performances of the three study cases would be different. Therefore, a model should be further developed, with the considerations of frost accumulation and refrigerant distribution for an ASHP unit with a multi-circuit outdoor coil.

(d) Compared with the previous experimental study, although the heat supply and energy consumption in Study Case 3 were both decreased 4.6 kJ, its defrosting duration was extended 1 s. Therefore, in consideration of the indoor thermal comfort requirements, this type of control strategy was not suggested in the application of ASHP units.

References

[1] Byun JS, Jeonb CD, Jung JH, Lee J. The application of photo-coupler for frost detecting in an air-source heat pump. Int J Refrig 2006;29(2):191–8.
[2] Wang W, Feng YC, Zhu JH, Li LT, Guo QC, Lu WP. Performances of air source heat pump system for a kind of mal-defrost phenomenon appearing in moderate climate conditions. Appl Energy 2013;112:1138–45.
[3] Wang W, Ma ZL, Jiang Y, Yang Y, Xu S, Yang Z. Field test investigation of a double-stage coupled heat pumps heating system for cold regions. Int J Refrig 2005;28(5):672–9.
[4] Yao Y, Jiang YQ, Deng SM, Ma ZL. A study on the performance of the airside heat exchanger under frosting in an air source heat pump water heater/chiller unit. Int J Heat Mass Transf 2004;47:17–8.
[5] Li LT, Wang W, Sun YY, Feng YC, Lu WP, Zhu JH, et al. Investigation of defrosting water retention on the surface of evaporator impacting the performance of air source heat pump during periodic frosting-defrosting cycles. Appl Energy 2014;135:98–107.
[6] Wang FH, Wang ZH, Zheng YX, Lin Z, Hao PF, Huan C, et al. Performance investigation of a novel frost-free air-source heat pump water heater combined with energy storage and dehumidification. Appl Energy 2015;139:212–9.
[7] Abdel-Wahed RM, Hifni MA, Sherif SA. Hot water defrosting of a horizontal flat plate cooling surface. Int J Refrig 1983;6:152–4.
[8] Huang D, Li QX, Yuan XL. Comparison between hot-gas bypass defrosting and reverse-cycle defrosting methods on an air-to-water heat pump. Appl Energy 2009;86(9):1697–703.
[9] Qu ML, Xia L, Deng SM, Jiang YQ. Improved indoor thermal comfort during defrost with a novel reverse-cycle defrosting method for air source heat pumps. Build Environ 2010;45(11):2354–61.
[10] Song MJ, Pan DM, Li N, Deng SM. An experimental study on the negative effects of downwards flow of the melted frost over a multi-circuit outdoor coil in an air source heat pump during reverse cycle defrosting. Appl Energy 2015;138:598–604.
[11] Song MJ, Deng SM, Pan DM, Mao N. An experimental study on the effects of downwards flowing of melted frost over a vertical multi-circuit outdoor coil in an air source heat pump on defrosting performance during reverse cycle defrosting. Appl Therm Eng 2014;67(1–2):258–65.
[12] Watters RJ, O'Neal DL, Yang JX. Frost/defrost performance of a three-row fin staged heat pump evaporator. ASHRAE Trans 2002;108(2):318–29.
[13] Hu WJ, Jiang YQ, Qu ML, Yao Y, Deng SM. An experimental study on the operating performance of a novel reverse-cycle hot gas defrosting method for air source heat pumps. Appl Therm Eng 2011;31(2):363–9.
[14] Qu ML, Xia L, Jiang YQ, Deng SM. A study of the reverse cycle defrosting performance on a multi-circuit outdoor coil unit in an air source heat pump – Part I: Experiments. Appl Energy 2012;91:122–9.
[15] Wang ZY, Wang XX, Dong ZM. Defrost improvement by heat pump refrigerant charge compensating. Appl Energy 2008;85:1050–9.
[16] Qu ML, Xia L, Deng SM, Jiang YQ. A study of the reverse cycle defrosting performance on a multi-circuit outdoor coil unit in an air source heat pump – Part II: Modeling analysis. Appl Energy 2012;91:274–80.
[17] Song MJ, Deng SM, Xia L. A semi-empirical modeling study on the defrosting performance for an air source heat pump unit with local drainage of melted frost from its three-circuit outdoor coil. Appl Energy 2014;136:537–47.
[18] Ameen FR, Coney JER, Sheppard CGW. Experimental study of warm-air defrosting of heat-pump evaporators. Int J Refrig 1993;16:13–8.
[19] Melo C, Knabben FT, Pereira PV. An experimental study on defrost heaters applied to frost-free household refrigerators. Appl Therm Eng 2013;51:239–45.
[20] Yin HJ, Yang Z, Chen AQ, Zhang N. Experimental research on a novel cold storage defrost method based on air bypass circulation and electric heater. Energy 2012;37:623–31.
[21] Kim J, Choi HJ, Kim KC. A combined Dual Hot-Gas Bypass Defrosting method with accumulator heater for an air-to-air heat pump in cold region. Appl Energy 2015;147:344–52.
[22] Hu B, Wang XL, Cao F, He ZL, Xing ZW. Experimental analysis of an air-source transcritical CO_2 heat pump water heater using the hot gas bypass defrosting method. Appl Therm Eng 2014;71:528–35.
[23] Krakow KI, Yan L, Lin S. A model of hot gas defrosting of evaporators, Part 1: Heat and mass transfer theory. ASHRAE Trans 1992;98(1):451–61.
[24] Krakow KI, Yan L, Lin S. A model of hot gas defrosting of evaporators, Part 2: Experimental analysis. ASHRAE Trans 1992;98(1):462–74.
[25] Alberto Dopazo J, Fernandez-Seara J, Uhía FJ, Diz R. Modeling and experimental validation of the hot-gas defrost process of an air-cooled evaporator. Int J Refrig 2010;33(4):829–39.
[26] Krakow KI, Lin S, Yan L. An idealized model of reversed-cycle hot gas defrosting of evaporators, Part 1: Theory. ASHRAE Trans 1993;99(2):317–28.

10

[27] Krakow KI, Lin S, Yan L. An idealized model of reversed-cycle hot gas defrosting of evaporators, Part 2: Experimental analysis and validation. ASHRAE Trans 1993;99(2):329–38.

[28] O'Neal DL, Peterson KT, Anand NK, Schliesing JS. Refrigeration system dynamics during the reversing cycle defrost. ASHRAE Trans 1998;95 (2):689–98.

[29] Young DJ. Development of a northern climate residential air-source heat pump. ASHRAE Trans 1980;86(1):671–86.

[30] Yang DK, Lee KS, Song S. Fin spacing optimization of a fin-tube heat exchanger under frosting conditions. Int J Heat Mass Transf 2006;49:2619–25.

[31] Cai L, Wang RH, Hou PX, Zhang XS. Study on restraining frost growth at initial stage by hydrophobic coating and hygroscopic coating. Energy Build 2011;43:1159–63.

[32] Mei VC, Gao Z, Tomlinson JJ. Frost-less heat pump. ASHRAE Trans 2002;108 (1):452–9.

[33] Song MJ, Wang ZH, Mao N, Li Z, Chen Y. An experimental study on the uneven refrigerant distribution over a vertically installed multi-circuit outdoor coil in an air source heat pump unit during reverse cycle defrosting. Appl Therm Eng 2015;91:975–85.